# A Density Functional Study of the $H_2O$−HOCO Complex

**Simone Aloisio and Joseph S. Francisco***

*Department of Chemistry and Department of Earth and Atmospheric Sciences, Purdue University, West Lafayette, Indiana 47907*

*Received: August 11, 1999; In Final Form: October 29, 1999*

We have calculated the structure of the complex between $H_2O$ and HOCO. The $H_2O$−HOCO complex has a relatively large binding energy of 7.1 kcal $mol^{-1}$ at the B3LYP/6-311++G(3df,3pd) level of theory. Structure and vibrational frequencies were also calculated. Infrared spectroscopy is a possible method for detection of this complex due to the large shifts in frequency and intensities relative to the parent monomers of fundamental modes in the complex. These data are used to calculate equilibrium constant for the formation of the complex, as well as rate constants for its dissociation. These data suggest the formation of the $H_2O$−HOCO complex may compete with HOCO dissociation in the OH + CO reaction in the presence of water.

## I. Introduction

The oxidation of carbon monoxide (CO) by the hydroxyl radical (OH) is an important reaction in the atmosphere and in combustion chemistry, influencing the chemistry of many key cycles.[1] The reaction involves an association complex,[2−4] HOCO, in a vibrationally excited state, from the following reaction scheme:

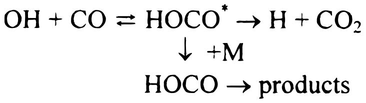

$$\begin{array}{c} OH + CO \rightleftharpoons HOCO^{*} \rightarrow H + CO_2 \\ \downarrow +M \\ HOCO \rightarrow \text{products} \end{array} \quad (1)$$

These channels lead to the formation of hydroperoxyl radical ($HO_2$) in the presence of $O_2$.[5,6] The formation of an association complex as an intermediate to this reaction leads to a pressure dependence of the rate constant for the formation of products. The magnitude of this pressure dependence also relies on what the collision partner (M) is. Many quasiclassical and quantum[7−9] calculations have been performed, elaborately detailing each of the steps in reaction 1. Experiments[10] show that when the collision partner is water ($M = H_2O$), it is 10 times as efficient a third body as $N_2$. There is uncertainty on whether the effective quenching of HOCO* by $H_2O$ may be affecting the results of recent studies[11] of the mass-independent fractionation (MIF) of oxygen in the reaction of carbon monoxide and hydroxyl radical. There is conflicting data concerning a dependence of the rate constant for this reaction and the concentration of water. At least one experimental study[12] finds that there is a water concentration dependence on this rate constant. The hydroperoxyl radical self-reaction rate constant shows a dependence on the water concentration present.[13,14] In that case, the dependence is due to the formation of a complex between $H_2O$ and $HO_2$. If there is a water dependence on the rate constant for reaction 1, a complex between $H_2O$ and HOCO may be formed as well.

The work that we present investigates the existence of a complex between $H_2O$ and HOCO. We calculate the structure, rotational constants, vibrational frequencies and energetics of this complex. We also examine the lifetime of the $H_2O$−HOCO complex and relate that to laboratory experiments previously performed.

## II. Computational Methods

All calculations were performed using the GAUSSIAN 94[15] suite of programs. Geometries were optimized using the Becke three-parameter hybrid functional combined with Lee, Yang, and Parr correlation [B3LYP][16] density functional theory method. This method has been shown to produce reliable results for hydrogen bonded complexes when compared with other methods.[17,18] Basis sets employed are the 6-31G(d), 6-311++G (d,p), 6-311++G (2d,2p), 6-311++G(2df,2p), and 6-311++G (3df,3pd). Frequency calculations were also performed at the B3LYP/6-311++G(3df,3pd) level of theory. Zero-point energies taken from these frequency calculations can be assumed to be an upper limit due to the anharmonic nature of the potential energy surface.

## III. Results and Discussion

The calculated structure, rotational constants, and harmonic vibrational frequencies for *cis*-HOCO are listed in Table 1. In the calculated lowest energy structure for HOCO, the four atoms are planar. There are two carbon−oxygen bonds. The shorter one between the carbon and the terminal oxygen ($C-O_2$) has a calculated bond distance of 1.181 Å at the highest level of theory used, B3LYP/6-311++G(3df,3pd). This is longer than what is calculated for either carbon monoxide or carbon dioxide at the same level of theory, which have bond distances of 1.125 and 1.159 Å, respectively. The other carbon−oxygen bond has a calculated distance of 1.323 Å.

The structure of $H_2O$−HOCO is shown in Figure 1. It has a six-membered ring structure including all the atoms except one of the hydrogens from water ($H_3$). These six atoms are nearly in plane, while $H_3$ is out of the plane by about 120°. The six atoms forming the ring are within 12° of being planar. The principle interaction is between the oxygen on the water ($O_3$) and the hydrogen on HOCO ($H_1$). This bond distance is calculated to be 1.731 Å at the B3LYP/6-311++G(3df,3pd) level of theory. There is also a slight interaction between one of the hydrogens on the water ($H_2$) and the terminal oxygen on HOCO ($O_2$). The distance between these two atoms is 2.338 Å at the highest level of theory. Evidence of these interactions is present in the altered geometry of HOCO when complexed with

10.1021/jp9928356 CCC: $19.00

**TABLE 1: Geometry, Rotational Constants, and Vibrational Frequencies (and Intensities) of HOCO**[a]

| | B3LYP | | | | |
|---|---|---|---|---|---|
| parameters | 6-31G(d) | 6-311++G(d,p) | 6-311++G(2d,2p) | 6-311++G(2df,2p) | 6-311++G(3df,3pd) |
| $H_1-O_1$ | 0.984 | 0.978 | 0.976 | 0.977 | 0.977 |
| $O_1-C$ | 1.331 | 1.326 | 1.325 | 1.323 | 1.323 |
| $C-O_2$ | 1.192 | 1.183 | 1.182 | 1.181 | 1.181 |
| $H_1-O_1-C$ | 108.9 | 109.8 | 109.6 | 110.0 | 109.8 |
| $O_1-C-O_2$ | 130.0 | 130.7 | 130.7 | 130.9 | 130.9 |
| $H_1-O_1-C-O_2$ | 0.0 | 0.0 | 0.0 | 0.0 | 0.0 |
| $A$ | 138383 | 142918 | 142952 | 144078 | 144004 |
| $B$ | 11721 | 11771 | 11789 | 11789 | 11809 |
| $C$ | 10806 | 10876 | 10891 | 10898 | 10914 |
| $\nu_1$ | 3514 (10.9) | 3586 (16.6) | 3592 (18.4) | 3583 (16.8) | 3579 (15.5) |
| $\nu_2$ | 1880 (281.1) | 1868 (373.20 | 1856 (345.3) | 1866 (350.1) | 1869 (340.6) |
| $\nu_3$ | 1311 (0.8) | 1284 (0.5) | 1304 (0.8) | 1292 (0.3) | 1294 (0.5) |
| $\nu_4$ | 1091 (152.9) | 1070 (172.5) | 1067 (170.4) | 1069 (167.7) | 1072 (164.7) |
| $\nu_5$ | 611 (122.0) | 599 (34.4) | 598 (31.1) | 598 (32.0) | 599 (31.6) |
| $\nu_6$ | 592 (34.6) | 580 (124.2) | 585 (110.7) | 583 (111.0) | 585 (106.8) |

[a] Bond distances and reported in angstroms, bond angles and dihedrals in degrees. Rotational Constants are reported in megahertz. Vibrational frequencies are reported in $cm^{-1}$, intensities in km $mol^{-1}$.

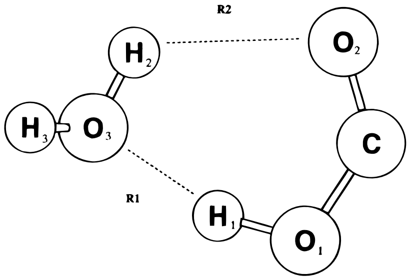

**Figure 1.** Structure of the $H_2O-HOCO$ complex.

water. Because of the strong interaction between the atoms labeled $O_3$ and $H_1$, the hydrogen−oxygen bond distance in HOCO ($H_1-O_3$) is the coordinate most affected by water complexation. In isolated HOCO, $H_1-O_3$ has a bond distance of 0.977 Å, while when complexed with water, this bond distance is 0.999 Å, a difference of 2.25%. The $O_1-C$ bond distance is shorter in the complex than in isolated HOCO by 1.22%. The increased $C-O_2$ bond distance in water complexed HOCO, 0.85%, is evidence for a slight interaction along the R2 coordinate. The complete geometry of $H_2O-HOCO$ is listed in Table 2. This can be compared to the geometry of similar complexes. $HO_2-H_2O$ has geometry similar to the $H_2O-HOCO$ complex.[19] It has a five-membered ring-like structure including all the atoms except one of the hydrogen atoms of water. The intermolecular bond distance of the principle hydrogen bond, analogous to R1, is 1.781 Å at the B3LYP/6-311++G(3df,3pd) level of theory. This is only slightly longer, 0.050 Å, than that of the $H_2O-HOCO$ complex. The $HO_3-H_2O$ has the same connectivity as the $H_2O-HOCO$ complex,[20] with the substitution of an oxygen atom for the carbon atom in HOCO. $H_2O-HOCO$ has a shorter hydrogen bond than $HO_3-H_2O$ as well, with the latter complex having an R1 distance of 1.781 Å at the same level of theory. The intermolecular distance between the terminal oxygen, $O_2$ in the case of $H_2O-HOCO$, and the in-plane hydrogen of the water, R2, is also shorter in $H_2O-HOCO$ than in the other two complexes. For the $HO_2-H_2O$ complex, R2 is 2.406 Å; while for $HO_3-H_2O$, this distance is 2.475 Å. These are about 3% and 6% longer than in $H_2O-HOCO$, respectively. The rotational constants for $H_2O-HOCO$, listed in Table 3, are consistent with the structure of the molecule. $H_2O-HOCO$ is an asymmetric rotor, with $A \neq B \neq C$.

The $H_2O-HOCO$ complex has 15 fundamental vibrational modes. Of these, three are similar to modes in isolated water, six are similar to those in isolated HOCO, and the remaining six modes are completely unique intermolecular modes. The modes that are similar to the isolated monomers are shifted with respect to the monomers due to changes in geometry induced by new interactions with other atoms present in the complex.

**TABLE 2: Geometry of $H_2O-HOCO$**[a]

| | B3LYP | | | | |
|---|---|---|---|---|---|
| coordinate | 6-31G(d) | 6-311++G(d,p) | 6-311++G(2d,2p) | 6-311++G(2df,2p) | 6-311++G(3df,3pd) |
| R1 | 1.708 | 1.742 | 1.740 | 1.745 | 1.731 |
| R2 | 2.108 | 2.401 | 2.340 | 2.345 | 2.338 |
| $H_1O_1$ | 1.012 | 0.998 | 0.998 | 0.998 | 0.999 |
| $O_1C$ | 1.312 | 1.311 | 1.310 | 1.309 | 1.307 |
| $CO_2$ | 1.205 | 1.193 | 1.192 | 1.192 | 1.191 |
| $H_3O_3$ | 0.971 | 0.963 | 0.962 | 0.962 | 0.962 |
| $H_2O_3$ | 0.978 | 0.967 | 0.967 | 0.967 | 0.967 |
| $H_3O_3H_2$ | 104.8 | 106.9 | 106.3 | 106.5 | 106.3 |
| $H_1O_1C$ | 107.7 | 108.5 | 108.3 | 108.6 | 108.5 |
| $O_1CO_2$ | 130.1 | 130.7 | 130.6 | 130.8 | 130.8 |
| $H_2O_3H_1$ | 92.2 | 102.1 | 97.0 | 97.5 | 97.2 |
| $O_3H_1O_1$ | 156.9 | 159.5 | 160.3 | 159.7 | 160.0 |
| $H_1O_1CO_2$ | −0.3 | 0.3 | −0.1 | −0.2 | −0.1 |
| $H_2O_3H_1O_1$ | −6.1 | 6.6 | 3.7 | 5.9 | 6.8 |
| $H_3O_3H_1O_1$ | 100.7 | 128.3 | 119.3 | 120.6 | 121.0 |
| $O_3H_1O_1C$ | 1.7 | −4.9 | −3.9 | −4.1 | −4.7 |

[a] Bond distances and reported in angstroms, bond angles and dihedrals in degrees.

**TABLE 3: Rotational Constants for $H_2O-HOCO$**[a]

| rotational constants | B3LYP | | | | |
|---|---|---|---|---|---|
| | 6-31G(d) | 6-311++G(d,p) | 6-311++G(2d,2p) | 6-311++G(2df,2p) | 6-311++G(3df,3pd) |
| *A* | 11593 | 11851 | 11871 | 11876 | 11913 |
| *B* | 5400 | 4991 | 4991 | 5001 | 5017 |
| *C* | 3724 | 3530 | 3544 | 3539 | 3554 |

[a] Rotational constants are reported in megahertz.

**TABLE 4: Vibrational Frequencies for $H_2O-HOCO$**[a]

| mode number | mode description | B3LYP/6-311++G(3df,3pd) | | |
|---|---|---|---|---|
| | | frequency | (shift) | intensity |
| 1 | $H_2-O_3-H_3$ asymmetric stretch | 3872 | (−41) | 104.1 |
| 2 | $H_2-O_3-H_3$ symmetric stretch | 3747 | (−67) | 52.7 |
| 3 | $H_1-O_1$ stretch | 3177 | (−402) | 723.3 |
| 4 | $C-O_2$ stretch | 1818 | (−51) | 339.7 |
| 5 | $H_2-O_3-H_3$ bend | 1623 | (−4) | 96.7 |
| 6 | $H_1-O_1-C$ bend | 1436 | (+142) | 14.7 |
| 7 | $C-O_1$ stretch | 1168 | (+96) | 160.9 |
| 8 | $H_1$ out-of-plane wag | 887 | (+302) | 117.3 |
| 9 | $O_1-C-O_2$ bend | 670 | (+71) | 18.3 |
| 10 | $H_2-O_3-H_1$ bend | 480 | | 141.0 |
| 11 | $H_2-O_3-H_3$ twist | 349 | | 101.3 |
| 12 | $O_3-H_1-O_1-C$ torsion | 248 | | 13.5 |
| 13 | $O_3-H_1$ stretch | 237 | | 31.1 |
| 14 | $H_3-O_3-H_1-O_1$ torsion | 208 | | 58.9 |
| 15 | $H_2-O_3-H_1-O_1$ torsion | 107 | | 18.9 |

[a] Vibrational frequencies are reported in $cm^{-1}$, intensities in km $mol^{-1}$.

**TABLE 5: Binding Energy of the $H_2O-HOCO$ Complex**[a]

| level of theory | binding energy | |
|---|---|---|
| | $D_e$ | $D_o$ |
| B3LYP/6-31G(d) | 15.0 | 12.0 |
| B3LYP/6-311++G(d,p) | 10.4 | 8.1 |
| B3LYP/6-311++G(2d,2p) | 9.6 | 7.2 |
| B3LYP/6-311++G(2df,2p) | 9.5 | 7.2 |
| B3LYP/6-311++G(3df,3pd) | 9.5 | 7.1 |

[a] Binding energies are reported in kcal $mol^{-1}$.

The modes, shifts, and intensities of $H_2O-HOCO$ are listed in Table 4. The $H_1-O_1$ stretch is the most shifted mode, 402 $cm^{-1}$ to the same mode in isolated HOCO. This reflects the change in geometry in the $H_1-O_1$ bond distance due to the strong interaction between $H_2O$ and HOCO in the complex. A similar red shift is seen in both $HO_2-H_2O$ (296 $cm^{-1}$)[19] and $HO_3-H_2O$ (346 $cm^{-1}$)[20] in the analogous modes of those molecules. There is also a large blue shift in the HOCO torsion mode, which is described as an out-of-plane wag by the hydrogen atom of HOCO. This mode is shifted by 302 $cm^{-1}$ in the complex with respect to the same mode in the isolated monomer. While there is no analogous mode for the $HO_2-H_2O$ complex, in $HO_3-H_2O$ there is. That shift is larger than in $H_2O-HOCO$ by 179 $cm^{-1}$. Both the water asymmetric and symmetric stretches are red shifted in the complex, by 41 and 67 $cm^{-1}$, respectively. There is a large shift in the $H-O-C$ bend of HOCO, 146 $cm^{-1}$ to the blue of the isolated molecule. The $C-O_1$ stretch and $C-O_2$ stretch both have a moderately shifted frequencies of 96 $cm^{-1}$ to the blue and 51 $cm^{-1}$ to the red of the isolated HOCO modes, respectively. This reflects the strengthening and weakening of these respective bonds in the complex. The $O-C-O$ bend in HOCO is also shifted moderately, 71 $cm^{-1}$ to the blue of the isolated molecule. Only the $H-O-H$ bend of water is relatively unaffected by the complexation of $H_2O$ and HOCO. Many of the bands in $H_2O-HOCO$ have large intensities. The strongest absorbing band is the $H_1-O_1$ stretch, with a calculated intensity of 723.3 km $mol^{-1}$. This is over 40 times larger than the same mode in isolated HOCO. The $C-O_2$ stretch is also very strongly absorbing, with an intensity of 339.7 km $mol^{-1}$ in the complex, compared to 340.6 in isolated HOCO. The $H_2O-HOCO$ complex has eight fundamental vibrational bands with intensities above 80 km $mol^{-1}$, meaning they should be strong absorbers. This and the large shifts from the parent monomers in many of these modes indicate that the infrared spectroscopy may be suitable for detection of this complex.

The $H_2O-HOCO$ complex is lower in energy than isolated $H_2O$ and HOCO by 9.5 kcal $mol^{-1}$ ($D_e$) at the B3LYP/6-311++G(3df,3pd) level of theory. When differences in zero-point-energy are included, the binding energy ($D_o$) of $H_2O-HOCO$ is 7.1 kcal $mol^{-1}$. A list of the binding energies calculated in this work for this complex is in Table 5. The binding energies seem consistent using the 6-311++G(2d,2p) basis set or higher. The basis set superposition error (BSSE) is estimated to be less than 0.2 kcal $mol^{-1}$. It is clear that the 6-31G(d) basis set is unreliable for this method, overpredicting the binding energy by as much as 69%. This complex is relatively strongly bound when compared to $HO_2-H_2O$ and $HO_3-H_2O$. $HO_2-H_2O$ has a predicted binding energy of 6.2 kcal $mol^{-1}$ at the same level of theory,[19] 0.9 kcal $mol^{-1}$ less than $H_2O-HOCO$. This difference is even larger when compared to $HO_3-H_2O$,[20] which has a binding energy of 4.9 kcal $mol^{-1}$.

By using the binding energy, thermodynamic data can be calculated for the following reaction:

$$H_2O + HOCO \rightleftarrows H_2O-HOCO \tag{2}$$

The enthalpy of formation for HOCO is taken from ref 21. Room temperature thermodynamic data for $H_2O$ is taken from NASA's JPL Publication 97-4.[21] These data are extrapolated to other temperatures using Kirchhoff's law,

$$\Delta H(T_2) - \Delta H(T_1) = \Delta C_p\, \Delta T \tag{3}$$

where $T$ is the temperature and $\Delta C_p$ is the difference in heat capacity at constant pressure of the substances whose enthalpy is being calculated to those of the elements in their natural state. Differences in heat capacities are assumed to be independent of temperature. Entropies are extrapolated to different temperatures using the following equation:

$$S(T_2) - S(T_1) = C_v \ln(T_2/T_1) \tag{4}$$

where $C_v$ is the heat capacity at constant volume. The enthalpies of formation ($\Delta H_f$) have been calculated for the complex at 200 K and at 300 K. The enthalpy of formation ($\Delta H_f$) for the $H_2O-HOCO$ complex is −119.1 and −122.1 kcal $mol^{-1}$ at 200 and 300 K, respectively. The entropy values ($S$) at 200 and 300 K are 68.7 and 75.9 cal $mol^{-1}$ $K^{-1}$. We can use these data to calculate an equilibrium constant ($K_{eq}$) for reaction 2. At 200 K, $K_{eq}$ is $2.3 \times 10^{-14}$ $cm^3$ $molecule^{-1}$, while at 300 K, it is $1.7 \times 10^{-16}$ $cm^3$ $molecule^{-1}$. This means that at equal concentrations of reactants, formation of the complex is thermodynamically favored by over 135 times at 200 K than at 300 K.

The dissociation constants ($k_{diss}$) for the complex can also be calculated using a method first developed by Troe,[22,23] and further shown to be effective by Patrick and Golden[24] for reactions of atmospheric importance. The dissociation constant can be described by the following equation:

$$k_{diss} = Z_{LJ}\,\rho(E_0)RT\,(Q_{vib})^{-1}\exp(-E_0R^{-1}T^{-1})F_EF_{anh}F_{rot} \quad (5)$$

where $Z_{LJ}$ is the Lennard-Jones collision frequency; $\rho(E_0)$ is the density of states; $R$ is the gas constant; $T$ is the temperature; $Q_{vib}$ is the vibrational partition function for the associated species; $E_0$ is the critical energy; $F_E$ (1.3 at 200 K, 1.5 at 300 K), $F_{anh}$ (1.2), and $F_{rot}$ (5.1 at 200 K, 3.2 at 300 K), which are correction terms for the energy dependence of the density of states, anharmonicity and rotation, respectively.

For the $H_2O$−HOCO complex, $k_{diss}$ is calculated to be $3 \times 10^{-14}$ $cm^3$ $molecule^{-1}$ $s^{-1}$ at 200 K and $5 \times 10^{-12}$ $cm^3$ $molecule^{-1}$ $s^{-1}$ at 300 K. This can be translated into a lifetime for a molecule using the following equation:

$$\tau = (k_{diss}[M])^{-1} \quad (6)$$

where $\tau$ is the lifetime and [M] is the total number density of molecules. In an experiment such as the one performed by Paraskevopoulos and Irwin,[10] a typical [M] used is $7 \times 10^{17}$ molecules $cm^3$. This means that the room-temperature lifetime of $H_2O$−HOCO would be about 300 ns at 300 K. Experiments were also run at much higher total number densities, $[M] \approx 2 \times 10^{19}$ molecules $cm^3$. Under these conditions, $\tau$ would be about 10 ns. At 200 K, these lifetimes increase to about 50 $\mu$s at the lower pressure and about 1.5 $\mu$s at the higher pressure.

The rate constant for the dissociation of HOCO has been investigated by Fulle et al.[4] In that work, it was shown that $k_{diss}$ for HOCO is on the order of $1 \times 10^{-13}$ $cm^3$ $molecule^{-1}$ $s^{-1}$. This includes decomposition to H + $CO_2$ and OH + CO. The values we calculate for the dissociation of the complex are comparable to this. This indicates that formation of $H_2O$−HOCO may compete with HOCO dissociation. The chemistry of $H_2O$−HOCO is, of course, unknown. However it is possible that this may have an effect on experiments in which HOCO is being produced in the presence of $H_2O$, such are those by Paraskevopoulos and Irwin,[10] Röckmann et al.,[11] and Beno et al.[12]

## IV. Conclusions

We have calculated the energetics, structure, and vibrational frequencies for the complex between $H_2O$ and HOCO. The $H_2O$−HOCO complex is at least as strongly bound as the complex between water and the hydroperoxyl radical. The $HO_2$−$H_2O$ complex is thought to be involved in the rate enhancement of the self-reaction of $HO_2$ in the presence of $H_2O$. There is some evidence for a water number density dependence on the rate of reaction between OH and CO. HOCO is a key intermediate in this reaction. It may be that $H_2O$−HOCO plays an important role in the OH + CO reaction in the presence of water.

**Acknowledgment.** The authors thank Brad Flowers for useful discussions that contributed to this work. The authors also thank the Jet Propulsion Laboratory for ample computing resources to carry out this research. The NASA Office of Space Science and Application sponsors the Jet Propulsion Laboratory Super-Computing Project.

## References and Notes

(1) Finlayson-Pitts, B. J.; Pitts, J. N., Jr. *Atmospheric Chemistry*; Wiley: New York, 1986.

(2) Smith, I. W. M. *Chem. Phys. Lett.* **1977**, *49*, 112.

(3) Mozurkewitch, M.; Lamb, J. J.; Benson, S. W. *J. Phys. Chem.* **1984**, *88*, 6435.

(4) Fulle, D.; Hamann, H. F.; Hippler, H.; Troe, J. *J. Chem. Phys.* **1996**, *105*, 983.

(5) DeMoore, W. B. *Int. J. Chem. Kinet.* **1984**, *16*, 1187.

(6) Miyoshi, A.; Matsui, H.; Washida, N. *J. Chem. Phys.* **1994**, *100*, 3532.

(7) Kudla, K.; Schatz, G. C.; Wagner, A. F. *J. Chem. Phys.* **1991**, *95*, 1635.

(8) Clary, D. C.; Schatz, G. C. *J. Chem. Phys.* **1993**, *99*, 4578.

(9) Goldfield, E. M.; Gray, S. K.; Schatz, G. C. *J. Chem. Phys.* **1995**, *102*, 8807.

(10) Paraskevopoulos, G.; Irwin, R. S. *J. Chem. Phys.* **1984**, *80*, 259.

(11) Röckmann, T.; Brenninkmeijer, C. A. M.; Saueressig, G.; Bergamaschi, P.; Crowley, J. N.; Fischer, H.; Crutzen, P. J. *Science* **1998**, *281*, 544.

(12) Beno, M. F.; Jonah, C. D.; Mulac, W. A. *Int. J. Chem. Kinet.* **1985**, *17*, 1091.

(13) Lii, R.-R.; Sauer, M. C., Jr.; Gordon, S. *J. Phys. Chem.* **1981**, *85*, 2833.

(14) Kircher, C. C.; Sander, S. P. *J. Phys. Chem.* **1984**, *88*, 2082.

(15) Frisch, M. J.; Trucks, G. W.; Schlegel, H. G.; Gill, P. M. W.; Johnson, B. G.; Robb, M. A.; Cheeseman, J. R.; Keith, T.; Petersson, G. A.; Montgomery, J. A.; Raghavachari, K.; Al-Laham, M. A.; Zakrzewski, V. G.; Ortiz, J. V.; Foresman, J. B.; Cioslowski, J.; Stefanov, B. B.; Nanayakkara, A.; Challacombe, M.; Peng, C. Y.; Ayala, P. Y.; Chen, W.; Wong, M. W.; Andres, J. L.; Replogle, E. S.; Gomperts, R.; Martin, R. L.; Fox, D. J.; Binkley, J. S.; Defrees, D. J.; Baker, J.; Stewart, J. P.; Head-Gordon, M.; Gonzalez, C.; Pople, J. A. *Gaussian 94*, revision D.2; Gaussian, Inc.: Pittsburgh, PA, 1995.

(16) Becke, A. M. *J. Chem. Phys.* **1993**, *98*, 5648.

(17) Kim, K.; Jordan, K. D. *J. Phys. Chem.* **1994**, *98*, 10089.

(18) Novoa, J. J.; Sosa, C. *J. Phys. Chem.* **1995**, *99*, 15837.

(19) Aloisio, S.; Francisco, J. S. *J. Phys. Chem.* **1998**, *102*, 1899.

(20) Aloisio, S.; Francisco, J. S. *J. Am. Chem. Soc.* **1999**, *121*, 8592.

(21) DeMore, W. B.; Sander, S. P.; Golden, D. M.; Hampson, R. F.; Kurylo, M. J.; Howard, C. J.; Ravishankara, A. R.; Kolb, C. E.; Molina, M. J. *Chemical Kinetics and Photochemical Data for Use in Stratospheric Modelling*, Evaluation No. 12; National Aeronautics and Space Administration-Jet Propulsion Laboratory: Pasadena, 1997.

(22) Troe, J. *J. Chem. Phys.* **1977**, *66*, 4745.

(23) Troe, J. *J. Chem. Phys.* **1977**, *66*, 4758.

(24) Patrick, R.; Golden, D. M. *Int. J. Chem. Kinetics* **1983**, *15*, 1189.